Al-Nahari, Azzam; Jantti, Riku; Sheikh, Muhammad Usman

Artificial Rich Scattering-Assisted MIMO Systems Using Passive Backscatter Devices

Published in:
2022 3rd Information Communication Technologies Conference, ICTC 2022

DOI:
10.1109/ICTC55111.2022.9778563

Published: 01/01/2022

Document Version
Peer-reviewed accepted author manuscript, also known as Final accepted manuscript or Post-print

Artificial Rich Scattering-Assisted MIMO Systems Using Passive Backscatter Devices

Azzam Al-nahari
Dpt. of Communications and Networking
Aalto University
Espoo, Finland
azzam.al-nahari@aalto.fi

Riku Jäntti
Dpt. of Communications and Networking
Aalto University
Espoo, Finland
riku.jantti@aalto.fi

Muhammad Usman Sheikh
Dpt. of Communications and Networking
Aalto University
Espoo, Finland
muhammad.sheikh@aalto.fi

***Abstract*—Reconfigurable intelligent surfaces (RIS) are emerging as a promising technology for the future 6G networks. One of the challenges of IRS systems is that they require feedback control which in turn means that they have to have receiver and microcontroller that consume power. In this paper, we propose to use passive chipless backscatter devices to shape the channel between the transmitter and the receiver. We propose a novel artificial rich scattering (ARS)-assisted MIMO system, that uses passive chipless backscatter devices to shape the channel covariance matrix by increasing its rank even if the direct transmission channel has strong line-of-sight (LoS) component. In particular, we conduct a large system analysis and show that the achievable rate is independent of the phase shift matrix at the backscattering nodes. Moreover, by introducing large number of passive scattering elements in the system, we can improve the system capacity even with the presence of strong LoS component in MIMO channel. We also consider the case of ARS-assisted MISO case when the channel state information (CSI) is available at the transmitter side and derive tight lower bound on the ergodic rate.**

***Index Terms*—Reconfigurable Intelligent Surfaces, Backscatter Communications, MIMO.**

I. Introduction

Reconfigurable intelligent surfaces (RIS) is believed to be a promising candidate technology for the sixth-generation (6G) networks [1]. Specifically, RIS is introduced as an extension of the traditional massive multiple-input-multiple-output (MIMO) systems retaining all the advantages of high spectral and energy efficiency, and with much lower energy consumption and deployment costs [2]. Typically, the RIS is deployed so that it yields a line of sight (LoS) paths with the transmitter and receiver. One of the main scenarios where RIS has gained a lot of attention recently is the improvement of spectral efficiency in multi-antenna systems [3], [4], [5] and references therein. For instance, the work in [4] derived a large system approximation of the ergodic rate in the RIS-assisted MIMO system. The ergodic spectral efficiency analysis of a single-stream RIS-assisted MIMO was investigated in [5].

One of the challenges of RIS is the need to feedback control [6], which implies that the RIS devices must be equipped with a transceiver and a microcontroller. Those increase the device complexity, cost, and power consumption. In addition, one of the main challenges of RIS-assisted wireless networks is the channel estimation for phase shift design, where reducing channel estimation overhead is still an open problem [7].

In this paper, we propose a new system based on large number of passive chipless backscatter devices. In particular, we investigate the performance of an artificial rich scattering (ARS) system that scatters the transmitted signals in order to shape the wireless channel for the MIMO system. Unlike in the single ARS node case studied in [8], the backscattering nodes do not send any information but re-scatter the transmitted signal. In addition, the direct channel in our system model is modeled as Rician channel in order to capture the effect of ARS nodes in enriching the direct propagation channel. Our approach is different from the above mentioned works related to RIS in two main aspects. First, in our work only passive backscattering nodes are leveraged to shape the channel without need of a controller for real time processing and optimizing the passive beamforming as in the RIS systems. Second, as the backscattering nodes can be distributed in a large area, the channels between both the transmitter and receiver and the scatterers can be modeled as as Rayleigh fading channel. This makes the effective channel of the ARS-assisted MIMO different from that using RIS, yet provide easier implementation and more favorable condition. We conduct large-antennas approximation and this is particularly beneficial in scenarios with massive MIMO deployment, where it is shown in [9] that considering massive antenna elements at the transmitter side can enhance both the spectral and energy efficiency of backscatter communication systems.

The main contributions of the paper are as follows. We propose an ARS-assisted MIMO system to enhance the system performance using chipless backscattering devices. We conduct large-system analysis of the achievable ergodic rate with large number of transmit antennas at the transmitter side. The ergodic rate is derived and the simulation results verify that the derived large-system approximation can provide accurate results for large-enough practical number of transmit antennas. It is shown the ergodic rate is independent on the phase shifts at the backscattering nodes. This is particularly important as our system setup do not have any input information related to the channel knowledge and hence the reflection coefficients matrix can not be optimized according to the instantaneous channel knowledge as in the case of RIS systems. Moreover,

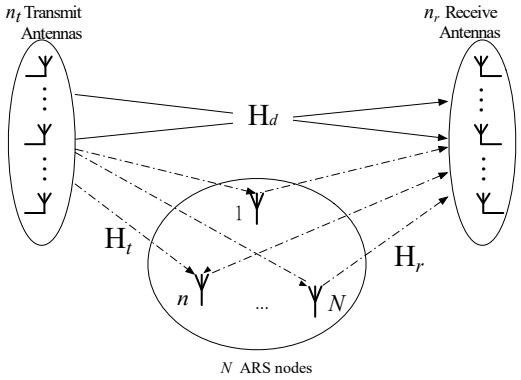

Fig. 1. Illustration of a ARS-assisted MIMO system.

we derive tight upper bound of the ergodic rate when the receiver has single antenna, i. e., ARS-assisted MISO case. It is also shown that the ergodic rate is independent on the phase shifts at the backscattering nodes even with arbitrary number of antennas at the transmitter side.

Notations: small and capital bold letters denote vectors and matrices, respectively; $\mathbf{I}$ and $\mathbf{0}$ denote an identity and zero matrices of appropriate size, respectively; denote the complex conjugate transpose and transpose of matrix $\mathbf{A}$ as $\mathbf{A}^{\dagger}$ and $\mathbf{A}^{\mathrm{T}}$, respectively.

II. System and channel models

Consider a single-user MIMO communication system that consists of an n_t-antenna transmitter and an n_r-antenna receiver as shown in Fig. 1. In addition, there is an ARS system comprises N single-antenna chipless backscatter nodes. Far field communication is assumed. In this setting, the information from the transmitter to the receiver propagate through two links, i.e., the direct links and links passing through the ARS nodes. For the analysis, we have adopted the following assumptions:

- (A1) the MIMO transmitter uses Gaussian codebook;
- (A2) the channel state information (CSI) is available at the receiver only for the case of ARS-assisted MIMO system. Moreover, the Rician factor of the channel is assumed not known at the transmitter [10];
- (A3) the channels are flat and quasi-static, i.e., there is no frequency selective fading;
- (A4) far-field assumption that the arriving waves look locally like plane waves.

These assumptions are applied also in previous works, for instance, [11]–[13] among others.

Let $h_{n,0i}$ denotes the complex link coefficient from antenna i of the TX to the backscatter object n. Moreover, let $h_{0j,n}$ be the complex link gain between the object n and antenna j of the RX. An ARS node n modulates the signal by imposing a phase shift $a_n = \zeta_n e^{i\theta_n}$, $n = 1, 2, \ldots, N$, where $\theta_n \in [2, \pi]$ and $\zeta_n \in [0, 1]$ denote the phase shift and amplitude reflection coefficient of the n-th backscatter node, respectively. Let $\mathbf{H}_t = [h_{n,0i}] \in \mathbb{C}^{N \times n_t}$ be the channel matrix between the transmitter and the objects, $\mathbf{H}_r = [h_{0j,n}] \in \mathbb{C}^{n_r \times N}$ be the channel matrix between the objects and the RX antennas. Both $\mathbf{H}_r$ and $\mathbf{H}_t$ contain independent and identical (i.i.d) distributed circularly symmetric complex Gaussian elements with zero mean and unit variance. Let $\mathbf{H}_d = [h_{0j,0i}] \in \mathbb{C}^{n_r \times n_t}$ denotes the channel matrix of the direct link, which is modeled as

$$\mathbf{H}_d = \sqrt{\frac{K}{K+1}}\bar{\mathbf{H}}_d + \sqrt{\frac{1}{K+1}}\widetilde{\mathbf{H}}_d, \tag{1}$$

in which $\mathbb{E}[\mathbf{H}_d] = \sqrt{\frac{K}{K+1}}\bar{\mathbf{H}}_d$, and K is the Rician factor, which represents the ratio between the deterministic and random energies. We assume that the channel matrix is given as $[\bar{\mathbf{H}}_d]_{ij} = 1$ for all i and j. $\widetilde{\mathbf{H}}_d = [h_{0j,0i}] \in \mathbb{C}^{n_r \times n_t}$ contains i.i.d standard circularly symmetric complex Gaussian elements with zero mean and unit variance. $\mathbf{H} \in \mathbb{C}^{n_r \times n_t}$ represents the effective channel matrix from the transmitter to the receiver and is given as follows

$$\mathbf{H} \triangleq \mathbf{H}_d + \mathbf{H}_r\mathbf{A}\mathbf{H}_t, \tag{2}$$

where $\mathbf{A} = \mathrm{diag}\{a_1, a_2, ..., a_N\}$ represents the diagonal phase-shifting matrix of the backscattering nodes. Note that the channel model in (2) has similar structure as that of RIS-assisted MIMO systems. However, in our case, the channel matrices $\mathbf{H}_t$ and $\mathbf{H}_r$ are modeled as Rayleigh fading, whereas in RIS-assisted MIMO systems, they are modeled as Rician fading channels [4], [5], [14], [15]. In addition, our approach in this paper is different from the RIS-assisted MIMO systems in that the backscatter nodes in our system setup do not have any input information related to the channel knowledge and hence the reflection coefficients represented by the matrix $\mathbf{A}$ can not be optimized according to the instantaneous channel knowledge as in the case of RIS systems.

The received signal vector at the receiver is given as

$$\mathbf{y} = \mathbf{H}\mathbf{x} + \mathbf{n}, \tag{3}$$

where $\mathbf{x} = [x_1, x_2, , ..., x_{n_t}]^{\mathrm{T}}$ is the transmit symbol vector, with $\mathbb{E}[\|\mathbf{x}\|^2] \leq P$, where P is the total average transmit power budget at the transmitter, and $\mathbf{n} = [n_j] \in \mathbb{C}^{n_r} \sim \mathcal{CN}(\mathbf{0}, \sigma_n^2\mathbf{I})$ is the additive white Gaussian noise (AWGN) at the receiver.

Considering that the CSI is available at the receiver side, and defining $\gamma \triangleq \frac{P}{\sigma_n^2}$, the achievable ergodic rate of the ARS-assisted MIMO system is given as [1]

$$R_{\mathrm{ARS}} = \mathbb{E}_{\mathbf{H}}\Big[\log_2 \det\Big(\mathbf{I} + \frac{\gamma}{n_t}\mathbf{H}\mathbf{H}^{\dagger}\Big)\Big]. \tag{4}$$

Maximizing the ergodic rate in (4) in terms of the phase shift matrix $\mathbf{A}$ is challenging since the ergodic rate involving expectation is too much complicated to be analyzed. Similar argument were presented in [4] and [5] for RIS-assisted MIMO systems. More importantly, real-time phase shift optimization

[1]The system can achieve this rate assuming that the elements of the matrix $\mathbf{A}$ is a known sequence at the receiver. This is a reasonable assumption as the ARS nodes act as a passive relays to assist the primary system.

at the passive backscattering nodes is not possible in practice, which is the main difference with the RIS systems, where an active controller is used for such task. To tackle this problem, we present a large system analysis approach for the proposed ARS-assisted MIMO system in the next section.

III. Achievable Rate: A large System Analysis

In this section, we conduct large-antenna approximation for the ergodic rate in (4) in order to get insights on the effect of the different system parameters on the performance. For comparison purpose, the achievable rate of the conventional MIMO system is also presented.

A. Conventional MIMO Channel

As a baseline, we will consider first the conventional point-to-point MIMO system, assuming perfect CSI is known only at the receiver. In this case, the channel model in (2) reduces to $\mathbf{H} = \mathbf{H}_d$, and thus the ergodic rate is given by

$$\begin{aligned} R_{\text{MIMO}} &= \mathbb{E}_{\mathbf{H}_d}\Big[\log_2\det\Big(\mathbf{I} + \frac{\gamma}{n_t}\mathbf{H}_d\mathbf{H}_d^\dagger\Big)\Big] \\ &= \mathbb{E}\Big[\log_2\det\Big(\mathbf{I} + \frac{\gamma}{n_t}\big(\frac{K}{K+1}\bar{\mathbf{H}}_d\bar{\mathbf{H}}_d^\dagger + \frac{\sqrt{K}}{K+1}\bar{\mathbf{H}}_d\widetilde{\mathbf{H}}_d^\dagger \\ &\quad + \frac{\sqrt{K}}{K+1}\widetilde{\mathbf{H}}_d\bar{\mathbf{H}}_d^\dagger + \frac{1}{K+1}\widetilde{\mathbf{H}}_d\widetilde{\mathbf{H}}_d^\dagger\big)\Big)\Big]. \end{aligned} \tag{5}$$

Note that $\lim_{n_t\to\infty}\frac{\widetilde{\mathbf{H}}_d\widetilde{\mathbf{H}}_d^\dagger}{n_t} = \mathbf{I}$, $\lim_{n_t\to\infty}\frac{\bar{\mathbf{H}}_d\widetilde{\mathbf{H}}_d^\dagger}{n_t} = \mathbf{0}$, and $\lim_{n_t\to\infty}\frac{\widetilde{\mathbf{H}}_d\bar{\mathbf{H}}_d^\dagger}{n_t} = \mathbf{0}$ [16]. Therefore, we obtain the ergodic rate of the large system approximation as follows

$$\widetilde{R}_{\text{MIMO}} = \log_2\det\Big(\mathbf{I} + \frac{K}{K+1}\frac{\gamma}{n_t}\bar{\mathbf{H}}_d\bar{\mathbf{H}}_d^\dagger + \frac{\gamma}{K+1}\mathbf{I}\Big). \tag{6}$$

It should be noted from (6) that $\lim_{K\to\infty}\widetilde{R}_{\text{MIMO}} = \log_2(1 + n_r\gamma)$, which corresponds to ergodic rate of the pure LoS MIMO channel [17], [10]. Moreover, $\lim_{K\to 0}\widetilde{R}_{\text{MIMO}} = n_r\log_2(1+\gamma)$, which is rate of the rich scattering Rayleigh channel [16]. Also, it can be seen that R_{MIMO} in (5) is a monotonically decreasing function of K for $K > 0$.

B. ARS-Assisted MIMO Channel

In this case, the achievable ergodic rate in (4) can be rewritten as

$$\begin{aligned} R_{\text{ARS}} &= \mathbb{E}_{\mathbf{H}}\Big[\log_2\det\Big(\mathbf{I} + \frac{\gamma}{n_t}\mathbf{H}\mathbf{H}^\dagger\Big)\Big] \\ &= \mathbb{E}_{\mathbf{H}}\Big[\log_2\det\Big(\mathbf{I} + \frac{\gamma}{n_t}\Big(\frac{K}{K+1}\bar{\mathbf{H}}_d\bar{\mathbf{H}}_d^\dagger \\ &\quad + \frac{\sqrt{K}}{K+1}\bar{\mathbf{H}}_d\widetilde{\mathbf{H}}_d^\dagger + \frac{\sqrt{K}}{K+1}\widetilde{\mathbf{H}}_d\bar{\mathbf{H}}_d^\dagger \\ &\quad + \frac{1}{K+1}\widetilde{\mathbf{H}}_d\widetilde{\mathbf{H}}_d^\dagger + \sqrt{\frac{K}{K+1}}\bar{\mathbf{H}}_d\mathbf{H}_t^\dagger\mathbf{A}^\dagger\mathbf{H}_r^\dagger \\ &\quad + \sqrt{\frac{1}{K+1}}\widetilde{\mathbf{H}}_d\mathbf{H}_t^\dagger\mathbf{A}^\dagger\mathbf{H}_r^\dagger + \sqrt{\frac{K}{K+1}}\mathbf{H}_r\mathbf{A}\mathbf{H}_t\bar{\mathbf{H}}_d^\dagger \\ &\quad + \sqrt{\frac{1}{K+1}}\mathbf{H}_r\mathbf{A}\mathbf{H}_t\widetilde{\mathbf{H}}_d^\dagger + \mathbf{H}_r\mathbf{A}\mathbf{H}_t\mathbf{H}_t^\dagger\mathbf{A}^\dagger\mathbf{H}_r^\dagger\Big)\Big)\Big]. \end{aligned} \tag{7}$$

We consider the case $n_t\to\infty$, whereas n_r and N are fixed. This case is a typical example of massive MIMO systems [16], and we have $\frac{\widetilde{\mathbf{H}}_d\widetilde{\mathbf{H}}_d^\dagger}{n_t}\to\mathbf{I}$, $\frac{\mathbf{H}_t\mathbf{H}_t^\dagger}{n_t}\to\mathbf{I}$, $\frac{\bar{\mathbf{H}}_d\widetilde{\mathbf{H}}_d^\dagger}{n_t}\to\mathbf{0}$, and $\frac{\mathbf{H}_t\widetilde{\mathbf{H}}_d^\dagger}{n_t}\to\mathbf{0}$. Without loss of generality, assuming that $\zeta_1 = \zeta_2 = ... = \zeta_N = \zeta$, we get $\mathbf{A}\mathbf{A}^\dagger = \zeta\mathbf{I}$. Substituting these results in (7), it follows that

$$\begin{aligned} \widetilde{R}_{\text{ARS}} =& \mathbb{E}_{\mathbf{H}_r}\Big[\log_2\det\Big(\mathbf{I} + \frac{K}{K+1}\frac{\gamma}{n_t}\bar{\mathbf{H}}_d\bar{\mathbf{H}}_d^\dagger \\ &+ \frac{\gamma}{K+1}\mathbf{I} + \zeta^2\gamma\mathbf{H}_r\mathbf{H}_r^\dagger\Big)\Big]. \end{aligned} \tag{8}$$

Let us denote $\lambda_i, i = 1, 2, ..., \min(n_r, N) \triangleq \Omega$ as the i-th unordered eigenvalue of the correlation matrix $\mathbf{H}_r\mathbf{H}_r^\dagger$. Thus, (8) can be rewritten as

$$\begin{aligned} \widetilde{R}_{\text{ARS}} =& \mathbb{E}_{\lambda_i}\Big[\log_2\Big(1 + \frac{K}{K+1}n_r\gamma + \frac{\gamma}{K+1} + \lambda_1\zeta^2\gamma\Big) \\ &+ \sum_{i=2}^{\Omega}\log_2\Big(1 + \frac{\gamma}{K+1} + \lambda_i\zeta^2\gamma\Big) \\ &+ (n_r - \Omega)\log_2\Big(1 + \frac{\gamma}{K+1}\Big)\Big]. \end{aligned} \tag{9}$$

Note that when $N > n_r$, the last term in the right hand side of (9) is zero. However, although increasing N beyond n_r does not improve the rank of the overall channel matrix $\mathbf{H}$, it does improve the channel matrix condition number, and thus enhance the performance as will be shown via simulation results in Section V.

IV. Ergodic Rate Analysis

In this section, we shall derive the analytical expression for the ergodic rate in (9). Following similar approach as proposed in [18] and [19], the ergodic capacity in (9) can be derived by considering a random selected eigenvalue λ as follows

$$\begin{aligned} \widetilde{R}_{\text{ARS}} =& \mathbb{E}_{\lambda}\Big[\log_2\Big(1 + \frac{K}{K+1}n_r\gamma + \frac{\gamma}{K+1} + \lambda\zeta^2\gamma\Big)\Big] \\ &+ \Omega\mathbb{E}_{\lambda}\Big[\log_2\Big(1 + \frac{\gamma}{K+1} + \lambda\zeta^2\gamma\Big)\Big] \\ &+ (n_r - \Omega)\log_2\Big(1 + \frac{\gamma}{K+1}\Big). \end{aligned} \tag{10}$$

The probability density function (PDF) of a randomly selected eigenvalue of the Wishart matrix $\mathbf{H}_r\mathbf{H}_r^\dagger$ with $n_r \leqslant N$ is given as [19]

$$\begin{aligned} f_\lambda(\lambda) = \frac{1}{n_r}\sum_{k=0}^{n_r-1}\sum_{l=0}^{k}\sum_{i=0}^{2l}\Bigg\{ &\frac{(-1)^i(2l)!\lambda^{N-n_r+i}e^{-\lambda}}{2^{2k-i}l!i!(N-n_r+l)!} \\ &\times\binom{2k-2l}{k-l}\binom{2N-2n_r+2l}{2l-i}\Bigg\}, \lambda \geqslant 0 \end{aligned} \tag{11}$$

The following theorem gives a closed-form expression for the ergodic rate given in (10).

Theorem 1. *The achievable ergodic rate of the ARS-assisted MIMO system in (4) can be asymptotically approximated as in (10), which is given in closed-form as*

$$\widetilde{R}_{\rm ARS} = \frac{1}{\ln 2}\Big(\ln(\theta_1) + \ln(\theta_2)\Omega + \mathcal{I}_1 + \Omega\mathcal{I}_2\Big) + (n_r - \Omega)\log_2(1 + \frac{\gamma}{K+1}) \tag{12}$$

where

$$\mathcal{I}_\varpi = \sum_{k=0}^{n_r-1}\sum_{l=0}^{k}\sum_{i=0}^{2l}\sum_{j=1}^{N-n_r+i+1} \frac{(-1)^i(2l)!\binom{2k-2l}{k-l}}{n_r 2^{2k-i} l!i!(N-n_r+l)!} \times \binom{2N-2n_r+2l}{2l-i}(\frac{\theta_\varpi}{\zeta^2\gamma})^{N-n_r+i+1-j}(N-n_r+i)! \times e^{\frac{\theta_\varpi}{\zeta^2\gamma}}\Gamma\Big(-N+n_r-i-1+j, \frac{\theta_\varpi}{\zeta^2\gamma}\Big), \varpi = 1, 2.$$

Proof: See Appendix A. ∎

Note that $\widetilde{R}_{\rm ARS}$ in (12) is not proportional to the phase shifts at the backscatter devices. The most likely cause of this phenomenon is that the scattered components keep spatial isotropy. Therefore, the phase shift can be set arbitrarily. The same observation was reported in [5] for RIS-assisted MIMO system with spatially uncorrelated Rayleigh channels.

V. ARS-ASSISTED MISO CASE

In this section, we consider ARS-assisted MISO case, where the receiver has single antenna, and derive an upper bound on the ergodic rate. Defining the channels as in Section II, let $\mathbf{h}_d = \sqrt{\frac{K}{K+1}}\bar{\mathbf{h}}_d + \sqrt{\frac{1}{K+1}}\widetilde{\mathbf{h}}_d \in \mathbb{C}^{1\times n_t}$ denotes the channel vector from the transmitter to receiver and $\mathbf{h}_r \in \mathbb{C}^{1\times N}$ the channel vector from the backscattering nodes to the receiver. Thus, the effective channel between the transmitter and

$$\mathbf{h} \triangleq \mathbf{h}_d + \mathbf{h}_r\mathbf{A}\mathbf{H}_t. \tag{13}$$

The received signal at the receiver is expressed as

$$y = \sqrt{P}(\mathbf{h}_d + \mathbf{h}_r\mathbf{A}\mathbf{H}_t)\mathbf{f}^\dagger x + n, \tag{14}$$

where $n \sim \mathcal{CN}(0,1)$ is the AWGN at the receive antenna and x is the information symbol satisfying $\mathbb{E}[|x|^2] = 1$ and $\mathbf{f} \in \mathbb{C}^{1\times n_t}$ is the beamforming vector satisfying $\|\mathbf{f}\|^2 = 1$. In order to obtain beamforming gain in MISO case, the CSI is assumed available at the transmitter [20]. Adopting maximum ratio transmitting (MRT) at the transmitter, the beamforming vector is defined as $\mathbf{f} = \frac{\mathbf{h}}{\|\mathbf{h}\|}$ and thus the ergodic rate of the ARS-assisted MISO case is given as

$$R_{\rm ARS,\,MISO} = \mathbb{E}\Big[\log_2(1 + \gamma\mathbf{h}\mathbf{h}^\dagger)\Big]. \tag{15}$$

According to Jensen's inequality, an upper bound $\bar{R}_{\rm ARS,\,MISO}$ on the ergodic achievable rate is given as

$$R_{\rm ARS,\,MISO} \le \bar{R}_{\rm ARS,\,MISO} = \log_2\Big(1 + \gamma\mathbb{E}[\mathbf{h}\mathbf{h}^\dagger]\Big). \tag{16}$$

The expectation in (16) is defined as follows

$$\begin{aligned}\mathbb{E}[\mathbf{h}\mathbf{h}^\dagger] = \mathbb{E}\Big[&\frac{K}{K+1}\bar{\mathbf{h}}_d\bar{\mathbf{h}}_d^\dagger + \frac{\sqrt{K}}{K+1}\bar{\mathbf{h}}_d\widetilde{\mathbf{h}}_d^\dagger \\ &+ \sqrt{\frac{K}{K+1}}\bar{\mathbf{h}}_d\mathbf{H}_t^\dagger\mathbf{A}^\dagger\mathbf{h}_r^\dagger + \frac{\sqrt{K}}{K+1}\widetilde{\mathbf{h}}_d\bar{\mathbf{h}}_d^\dagger \\ &+ \frac{1}{K+1}\widetilde{\mathbf{h}}_d\widetilde{\mathbf{h}}_d^\dagger + \sqrt{\frac{1}{K+1}}\widetilde{\mathbf{h}}_d\mathbf{H}_t^\dagger\mathbf{A}^\dagger\mathbf{h}_r^\dagger \\ &+ \sqrt{\frac{K}{K+1}}\mathbf{h}_r\mathbf{A}\mathbf{H}_t\bar{\mathbf{h}}_d^\dagger + \sqrt{\frac{1}{K+1}}\mathbf{h}_r\mathbf{A}\mathbf{H}_t\widetilde{\mathbf{h}}_d^\dagger \\ &+ \mathbf{h}_r\mathbf{A}\mathbf{H}_t\mathbf{H}_t^\dagger\mathbf{A}^\dagger\mathbf{h}_r^\dagger\Big].\end{aligned} \tag{17}$$

Since the channel vectors are independent, the expectations of all terms are zeros except the first term, fifth term, and last term in (17). These terms are given as

$$\mathbb{E}\Big[\frac{K}{K+1}\bar{\mathbf{h}}_d\bar{\mathbf{h}}_d^\dagger\Big] = \frac{n_t K}{K+1} \tag{18}$$

$$\mathbb{E}\Big[\frac{1}{K+1}\widetilde{\mathbf{h}}_d\widetilde{\mathbf{h}}_d^\dagger\Big] = \frac{n_t}{K+1} \tag{19}$$

$$\mathbb{E}\Big[\mathbf{h}_r\mathbf{A}\mathbf{H}_t\mathbf{H}_t^\dagger\mathbf{A}^\dagger\mathbf{h}_r^\dagger\Big] = \zeta^2 n_t N \tag{20}$$

Substituting (17)-(20) into (16) we get

$$\bar{R}_{\rm ARS,\,MISO} = \log_2\Big(1 + \gamma n_t(\zeta^2 N + 1)\Big). \tag{21}$$

Again, we notice from (21) that the ergodic rate is independent of the phase shifts at the backscattering nodes. Moreover, interestingly, the asymptotic achievable rate of the MISO case is independent of Rician factor K.

VI. NUMERICAL RESULTS

In this section, we evaluate the performance of the considered system setup via simulations and numerical results. The large system approximation result in (12) is compared with the Monte-Carlo simulation results of the achievable ergodic rate in (4). Unless otherwise stated, we set $\gamma = 10$dB, $n_r = 4$, and $\zeta = 0.1$.

In Fig. 2, the ergodic rate is plotted versus the transmit SNR γ for different values of the Rician factor K. It is seen that the performance of ARS-assisted MIMO is better than that without ARS and better gain is obtained with $K = 0$ compared to $K = 10$. With $K = 0$, which corresponds to the case of pure Rayleigh channel, higher number of backscattering nodes are required to see a considerable improvement as the channel matrix is already full rank. Note also that the simulation results match well with the numerical results of the large-antennas approximation.

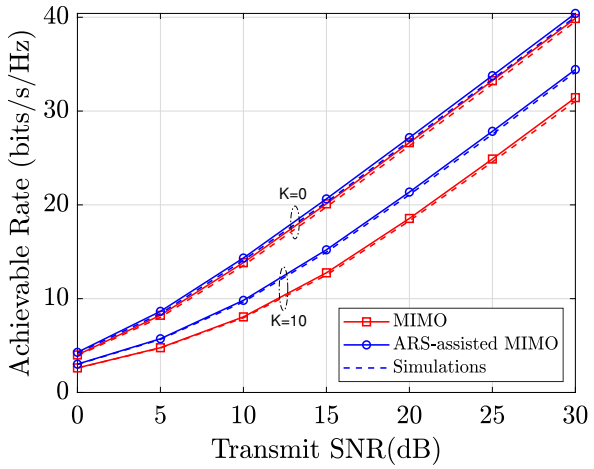

Fig. 2. Achievable rate versus the SNR γ, with $n_t = 32$, $n_r = 4$, $N = 10$, $\alpha = 0.1$, and different values of K.

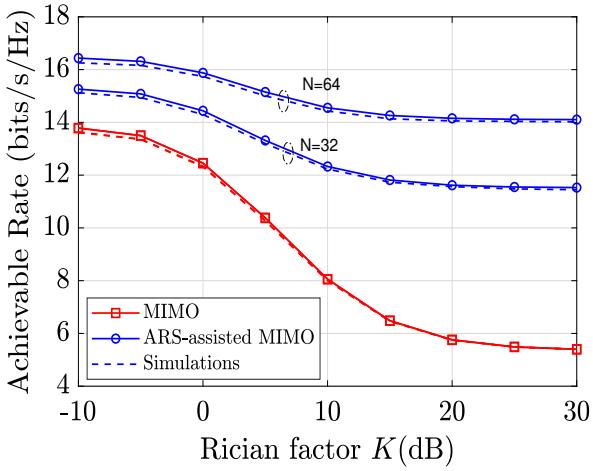

Fig. 4. Achievable rate versus Rician factor K , with $n_t = 64$, $n_r = 4$, $\alpha = 0.1$, $\gamma = 10$dB, and different values of N.

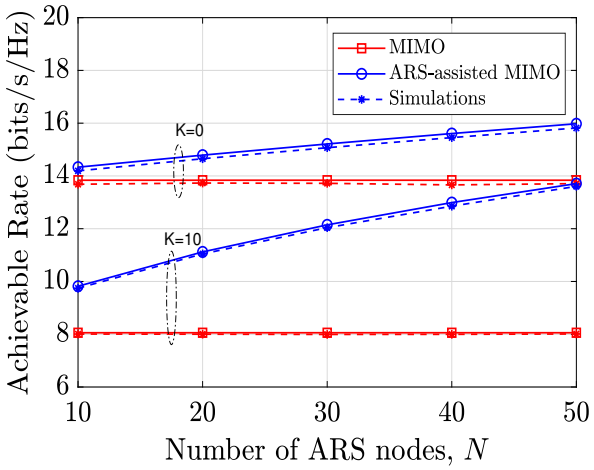

Fig. 3. Achievable rate versus the number of ARS nodes N, with $n_t = 64$, $n_r = 4$, $\alpha = 0.1$, $\gamma = 10$dB, and different values of K.

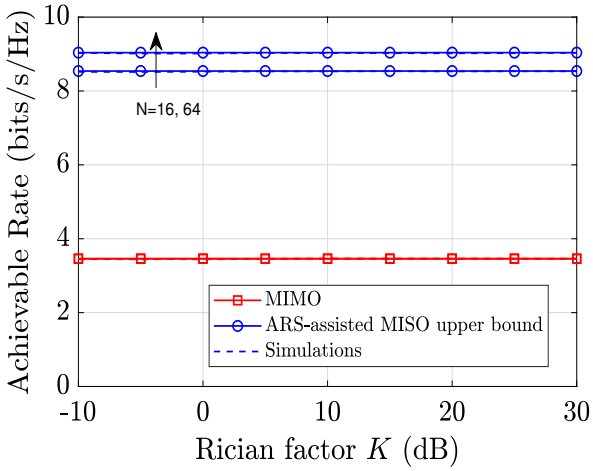

Fig. 5. Achievable rate versus Rician factor K for ARS-assisted MISO case, with $n_t = 32$, $n_r = 1$, $\alpha = 0.1$, $\gamma = 10$dB, and different values of N.

Fig. 3 shows the effect of increasing the number ARS nodes on the performance. We observe that the ergodic rate improves significantly with the number ARS nodes. This indicates that the larger number of backscattering nodes are distributed, the higher gain of the ARS-assisted MIMO system we can get. Note also that when the Rician factor increases, i.e., $K = 10$, this advantage is further enlarged. The figure also shows the tightness of the large-antenna approximation with the Monte Carlo results.

Fig. 4 shows the effect of increasing the Rician factor K on the performance. First notice the capacity degradation of the Rician channel as K increases. However, the gain of ARS-assisted MIMO over direct transmission increases as K increases. Furthermore, we observe that the ergodic rate improves significantly when the number of ARS nodes N increases from 32 to 64. Note that the effect of increasing the Rician factor diminishes as the number of ARS nodes increases. This demonstrates the effect ARS for improving the rank of the channel matrix leading to substantial capacity gains.

Fig. 5 shows the performance of the ARS-assisted MISO system. As shown in the figure, the upper bound is tightly closed with the Monte Carlo results. Interestingly, the ergodic rate is independent of the Rician factor as discussed in Section V. Another important observation is that increasing the number of backscattering nodes from 16 to 64 makes only slight improvement in the ergodic rate. This suggests using multiple antennas at the receiver in order to cultivate considerable gain from the proposed ARS system setup.

VII. Conclusion

In this paper, we introduced an ARS-assisted MIMO system to shape the channel matrix for improving the achievable rate. The proposed system setup enriches the propagation channel

of the MIMO system even if direct link has low rank. We analyzed the ergodic rate of ARS-assisted MIMO systems considering large-antenna approximation. It was shown that the ergodic rate is independent of the phase shift matrix at the backscattering nodes. The proposed system setup sheds light on the possible application of backscatter communications in scenarios such as massive MIMO systems with unfavorable channel condition between the transmitted and receiver. We also derived tight upper bound of the ergodic rate for the ARS-assisted MISO system and it it was concluded that having multiple antennas at the receiver is important to obtain high gain from the proposed ARS system.

APPENDIX A
PROOF OF THEOREM 1

Considering (11), and defining $\theta_1 \triangleq 1 + \frac{K}{K+1} n_r \gamma + \frac{\gamma}{K+1}$, and $\theta_2 \triangleq 1 + \frac{\gamma}{K+1}$, the ergodic rate of the ARS-assisted MIMO in (10) is given as

$$\begin{aligned}\widetilde{R}_{\mathrm{ARS}} &= \frac{1}{\ln 2} \int_0^\infty \ln(\theta_1 + \zeta^2 \gamma \lambda) f_\lambda(\lambda) d\lambda \\ &+ \frac{\Omega}{\ln 2} \int_0^\infty \ln(\theta_2 + \zeta^2 \gamma \lambda) f_\lambda(\lambda) d\lambda \\ &+ (n_r - \Omega) \log_2(1 + \frac{\gamma}{K+1}). \end{aligned} \tag{22}$$

After some trivial mathematical manipulation, (22) can be rewritten as

$$\begin{aligned}\widetilde{R}_{\mathrm{ARS}} &= \frac{\ln(\theta_1)}{\ln 2} + \frac{1}{\ln 2} \underbrace{\int_0^\infty \ln(1 + \frac{\zeta^2 \gamma}{\theta_1} \lambda) f_\lambda(\lambda) d\lambda}_{\mathcal{I}_1} \\ &+ \frac{\ln(\theta_2)\Omega}{\ln 2} + \frac{\Omega}{\ln 2} \underbrace{\int_0^\infty \ln(1 + \frac{\zeta^2 \gamma}{\theta_2} \lambda) f_\lambda(\lambda) d\lambda}_{\mathcal{I}_2} \\ &+ (n_r - \Omega) \log_2(1 + \frac{\gamma}{K+1}). \end{aligned} \tag{23}$$

Now, using (11), the integral $\mathcal{I}_1$ is solved as

$$\begin{aligned}\mathcal{I}_1 &= \frac{1}{n_r} \sum_{k=0}^{n_r-1} \sum_{l=0}^{k} \sum_{i=0}^{2l} \frac{(-1)^i (2l)! \binom{2k-2l}{k-l} \binom{2N-2n_r+2l}{2l-i}}{2^{2k-i} l! i! (N-n_r+l)!} \\ &\times \int_0^\infty \ln(1 + \frac{\zeta^2 \gamma}{\theta_1} \lambda) \lambda^{N-n_r+i} e^{-\lambda} d\lambda \\ &= \sum_{k=0}^{n_r-1} \sum_{l=0}^{k} \sum_{i=0}^{2l} \sum_{j=1}^{N-n_r+i+1} \frac{(-1)^i (2l)! \binom{2k-2l}{k-l}}{n_r 2^{2k-i} l! i! (N-n_r+l)!} \\ &\times \binom{2N-2n_r+2l}{2l-i} (\frac{\theta_1}{\zeta^2 \gamma})^{N-n_r+i+1-j} (N-n_r+i)! \\ &\times e^{\frac{\theta_1}{\zeta^2 \gamma}} \Gamma(-N+n_r-i-1+j, \frac{\theta_1}{\zeta^2 \gamma}), \end{aligned} \tag{24}$$

where the second equality in (24) is obtained by substituting $z \triangleq \frac{\zeta^2 \gamma}{\theta_1} \lambda$ and using [21, Eq. (4.222.8)] for solving the integral. Moreover, $\mathcal{I}_2$ can be obtained in a similar way. Substituting for $\mathcal{I}_1$ and $\mathcal{I}_1$ into (23), (12) is obtained.

REFERENCES

[1] J. Zhang, E. Björnson, M. Matthaiou, D. W. K. Ng, H. Yang, and D. J. Love, "Prospective multiple antenna technologies for beyond 5G," *IEEE J. Sel. Areas Commun.*, vol. 38, no. 8, pp. 1637–1660, 2020.

[2] S. Hu, F. Rusek, and O. Edfors, "Beyond massive MIMO: The potential of data transmission with large intelligent surfaces," *IEEE Trans. Signal Process.*, vol. 66, no. 10, pp. 2746–2758, 2018.

[3] Y. Liu, X. Liu, X. Mu, T. Hou, J. Xu, M. Di Renzo, and N. Al-Dhahir, "Reconfigurable intelligent surfaces: Principles and opportunities," *IEEE Commun. Surveys Tuts.*, vol. 23, no. 3, pp. 1546–1577, 2021.

[4] J. Zhang, J. Liu, S. Ma, C.-K. Wen, and S. Jin, "Large system achievable rate analysis of RIS-assisted MIMO wireless communication with statistical CSIT," *IEEE Trans. Wireless Commun.*, vol. 20, no. 9, pp. 5572–5585, 2021.

[5] J. Wang, H. Wang, Y. Han, S. Jin, and X. Li, "Joint transmit beamforming and phase shift design for reconfigurable intelligent surface assisted MIMO systems," *IEEE Trans. Cogn. Commun. Netw.*, vol. 7, no. 2, pp. 354–368, 2021.

[6] E. Björnson, Ö. Özdogan, and E. G. Larsson, "Reconfigurable intelligent surfaces: Three myths and two critical questions," *IEEE Commun. Magazi*, vol. 58, no. 12, pp. 90–96, 2020.

[7] C. Pan, H. Ren, K. Wang, J. F. Kolb, M. Elkashlan, M. Chen, M. Di Renzo, Y. Hao, J. Wang, A. L. Swindlehurst, X. You, and L. Hanzo, "Reconfigurable intelligent surfaces for 6G systems: Principles, applications, and research directions," *IEEE Commun. Mag.*, vol. 59, no. 6, pp. 14–20, 2021.

[8] R. Duan, R. Jäntti, H. Yiğitler, and K. Ruttik, "On the achievable rate of bistatic modulated rescatter systems," *IEEE Trans. Veh. Technol.*, vol. 66, no. 10, pp. 9609–9613, 2017.

[9] A. Al-Nahari, R. Jäntti, D. Mishra, and J. Hämäläinen, "Massive MIMO beamforming in monostatic backscatter multi-tag networks," *IEEE Commun. Lett.*, vol. 25, no. 4, pp. 1323–1327, 2021.

[10] S. K. Jayaweera and H. V. Poor, "On the capacity of multiple-antenna systems in Rician fading," *IEEE Trans. on Wireless Commun.*, vol. 4, no. 3, pp. 1102–1111, 2005.

[11] S. Loyka and G. Levin, "On physically-based normalization of MIMO channel matrices," *IEEE Trans. Wireless Commun.*, vol. 8, no. 3, pp. 1107–1112, Mar. 2009.

[12] G. Levin and S. Loyka, "From multi-keyholes to measure of correlation and power imbalance in MIMO channels: Outage capacity analysis," *IEEE Trans. Inf. Theory*, vol. 57, no. 6, pp. 3515–3529, Jun. 2011.

[13] D. Darsena, G. Gelli, and F. Verde, "Modeling and performance analysis of wireless networks with ambient backscatter devices," *IEEE Trans. Commun.*, vol. 65, no. 4, pp. 1797–1814, 2017.

[14] Ö. Özdogan, E. Björnson, and E. G. Larsson, "Using intelligent reflecting surfaces for rank improvement in mimo communications," in *IEEE International Conference on Acoustics, Speech and Signal Processing (ICASSP)*, 2020, pp. 9160–9164.

[15] S. Zhang and R. Zhang, "Capacity characterization for intelligent reflecting surface aided MIMO communication," *IEEE J. Sel. Areas Commun.*, vol. 38, no. 8, pp. 1823–1838, 2020.

[16] F. Rusek, D. Persson, B. K. Lau, E. G. Larsson, T. L. Marzetta, O. Edfors, and F. Tufvesson, "Scaling up MIMO: Opportunities and challenges with very large arrays," *IEEE Signal Process. Magaz.*, vol. 30, no. 1, pp. 40–60, 2013.

[17] G. Lebrun, M. Faulkner, M. Shafi, and P. Smith, "MIMO Ricean channel capacity: an asymptotic analysis," *IEEE Trans. Wireless Commun.*, vol. 5, no. 6, pp. 1343–1350, 2006.

[18] I. E. Telatar, "Capacity of multi-antenna gaussian channels," *European Trans. Telecommun.*, 1999.

[19] H. Shin and J. H. Lee, "Closed-form formulas for ergodic capacity of MIMO Rayleigh fading channels," in *IEEE International Conference on Communications, 2003. ICC '03.*, vol. 5, 2003, pp. 2996–3000.

[20] Y. Han, W. Tang, S. Jin, C.-K. Wen, and X. Ma, "Large intelligent surface-assisted wireless communication exploiting statistical CSI," *IEEE Trans. Veh. Technol.*, vol. 68, no. 8, pp. 8238–8242, 2019.

[21] I. S. Gradshteyn and I. M. Ryzhik, *Table of Integrals, Series, and Products*, 7th ed. New York, NY, USA: Elsevier, 2007.